



Improved Efficiency by the Effect of Strain on the Structure of a Solar Cell Based on GaInP/GaAs

A. Aissat^{1,2,3*}, R. Bestam¹, J.P. Vilcot³

LATSI Laboratory, Faculty of technology, University of Blida, BP270, 09.000, Algeria ¹

LASICOM Laboratory, Faculty of Sciences, University of Blida, BP270, 09.000, Algeria ²

Institut d'Electronique, de Microélectronique et de Nanotechnologie, UMR CNRS 8520, Université des Sciences et Technologies de Lille 1, Avenue Poincaré, CS 60069, 59652 Villeneuve d'Ascq, France ³

ABSTRACT: This work is aimed at the study of GaInP-based photovoltaic cell. The effects of In content, lattice parameter mismatch and thickness of the SiO₂ insulating layer on the characteristics and efficiency of the GaInP structure were investigated. We noticed that for higher In concentrations, the band gap energy decreases significantly. The structure possesses two different regions that are dopant concentration-dependent ($x < 0.48$ and $x > 0.48$). In the extensive strain region of $x < 0.48$, we found that the efficiency reaches 17.93% in a lattice-matched ($\delta = 5\text{nm}$) case. For a concentration $x > 0.48$, we have a compressive strain $\varepsilon > 0$ which leads to a higher efficiency. For $x = 0.9$, $\delta = 5\text{nm}$ and a strain of 3.3%, we achieved an efficiency of 26.6%. The results show that light conversion efficiency has considerably boosted by varying insulating layer thickness and strain values.

Keywords: III-V Semiconductors, Solar cells, Optoelectronic.

I. INTRODUCTION

Solar energy is extensively studied as an endless, reliable and safe energy source. It is particularly important to increase the photovoltaic (PV) conversion efficiency from the viewpoints of both basic science and practical applications. [1]. The InGa_{1-x}N alloy system offers a unique opportunity to develop high efficiency multi-junction solar cells. A single junction solar cells made of In_xGa_{1-x}N have been successfully developed, with $x = 0, 0.2, \text{ and } 0.3$. The materials are grown on sapphire substrates by molecular beam epitaxy (MBE). The structure consists of a Si-doped InGa_{1-x}N layer, an intrinsic layer and an Mg-doped InGa_{1-x}N layer on the top [2]. In_xGa_{1-x}N alloys possess a bandgap ranging from the near infrared (0.7eV) to the ultra violet (3.4eV) [3]. This range corresponds very closely to the solar spectrum one making In_xGa_{1-x}N alloys promising candidates for radiation-resistant multi-junction solar cells [4].

Materials with a bandgap energy $E_g < 1.4 \text{ eV}$ grown on GaAs substrates are of major interest for optoelectronic devices like multi-junction solar cells [5], 1.3 μm wavelength emitting lasers [6]. The ternary Ga_{1-x}In_xAs is an attractive material with a bandgap ranging from 1.44 eV for GaAs decreasing to 0.35 eV for InAs. Unfortunately, the lattice constant of this material also changes significantly when we modify the composition. Besides, lattice-matched substrates are not available for most Ga_{1-x}In_xAs compounds. This letter is the first report on the successful deposition of Ga_{0.35}In_{0.65}P/Ga_{0.83}In_{0.17}P tandem solar cells grown lattice mismatched to the GaAs substrate material. Even though the amount of dislocations was determined to be in the order of 10^7 cm^{-2} ; an excellent electrical performance of the device was achieved. The quantum efficiency was comparable to the lattice matched Ga_{0.51}In_{0.49}P/GaAs tandem solar cells [7]. GaInP/GaAs tandem cells currently represent the highest efficiency monolithic solar cells and are in commercial production for space applications [8]. Strained semiconductors can be successfully incorporated into photovoltaic devices, as long as the critical thickness is respected for each separate layer as for the whole structure [9].

Metal/semiconductors heterojunctions (SC) and SC A/SC B have a great impact on the realized PV solar cells. The electronic structure of the interface determines the electronic behavior of heterojunctions and Schottky barrier height



International Journal of Advanced Research in Electrical, Electronics and Instrumentation Engineering

(An ISO 3297: 2007 Certified Organization)

Vol. 3, Issue 1, January 2014

[10]. In our work, we have used indium/gallium-based compounds to prepare our structures. With these materials we are able to prepare different alloys by adding III-V compounds. Ternary alloys like $\text{Ga}_{(1-x)}\text{In}_x\text{P}$ and $\text{In}_x\text{As}_{(1-x)}\text{P}$ or quaternary compound like $\text{In}_x\text{Ga}_{(1-x)}\text{As}_y\text{P}_{(1-y)}$. In this type of materials, the forbidden band width could be changed which means that optical properties could be altered and improved at a certain spectral wavelengths range.

II. THEORY

III-V semiconductors like GaAs and InP tend to have a sphalerite (Zinc blende) structure when they crystallize. This type of structure is made exclusively of III-V atoms where we will have, stoichiometrically, one atom from column III elements corresponding to another atom from column V elements. As a result, strong covalent chemical bonds are obtained when one electron is shared between the atoms belonging to the group III elements and those of group IV. These bonds exhibit also weak ionic characteristics resulting from a difference in electronegativity between elements of group III and group IV. Let the lattice parameter 'a' be the distance between two adjacent lattices. For alloys made of different semiconductor materials, the lattice parameter varies linearly with the different binary elements composition in accordance with Vegard law. For ternary elements $\text{Ga}_{1-x}\text{In}_x\text{P}$, the lattice parameter a_{InGaP} is given by equation [11].

$$a_{\text{Ga}_{(1-x)}\text{In}_x\text{P}} = xa_{\text{InP}} + (1 - x)a_{\text{GaP}} \quad (1)$$

Semiconductors are characterized by an energy gap separating the conduction band from the valence band. This gap, called forbidden band, correspond to the energy needed for an electron to jump from the valence band to the conduction band. This energy could come from incident photons or electric excitations. This gap energy is equivalent to the energy provided by the system after the electron-hole recombination. The emission and detection phenomenon of photons is based on the detection of photons. When a material is grown on a substrate and if they possess different lattice parameters, there will be a parametric disagreement between the two lattices. This could be addressed depending on two cases:

1. If the grown films are very thin, their lattice will be distorted elastically in a manner where the material lattice parameter will fit with the substrate's one in a direction parallel to the interface. In the direction perpendicular to the growth interface, the lattice will be distorted either by having either an elongation or a contraction depending if the thin film lattice parameter is smaller or bigger than the substrate's one respectively. In this case, the layer is being totally strained.
2. For a thick epitaxial layer, the distortion of the material's lattice is not sufficient to balance the mechanical energy and stress generated during the thin film growth. This disagreement is compensated by dislocation generated at the interface during the growth. These dislocations will spread from the substrate to the growth interface followed by a layer relaxation.

We have used Van and Walle model and Krijin formalism [12] to describe the effect of this strain-related phenomenon. The consequences of the constraints on the valence band and conduction band could be divided in two parts:

- Hydrostatic component: it is related to the strain along the growth axis. It induces a shift in the center of gravity for both the valence band and the conduction band.
- Shear component: it leads to the lifting and increase in the degenerate energy levels for light and heavy holes at $\text{K}=0$.

International Journal of Advanced Research in Electrical, Electronics and Instrumentation Engineering

(An ISO 3297: 2007 Certified Organization)

Vol. 3, Issue 1, January 2014

III. SOLAR CELL STRUCTURE

We have realized a solar cell using N-type $Ga_{(1-x)}In_xP$ epitaxially grown on P-type GaAs. We have followed by the deposition of a thin Tin oxide (SnO_2) film that replaces the metal layer and acts as window layer and antireflective coating due to its interesting optoelectronic characteristics (gap = 3.6 eV, refractive index 1.9-2.0). the last step is the deposition of silicon (Si) thin layer which have a large forbidden band of 9eV with a high resistivity of ($10^{16}\Omega.cm$) that gives her good insulating properties (Fig. 1).

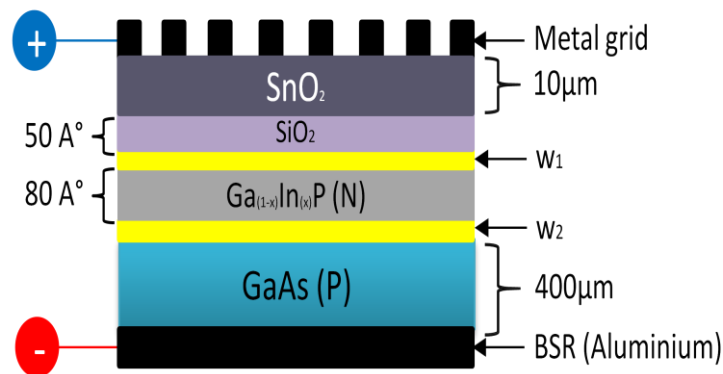


Fig. 1 Structure of the studied solar cell (type MIS)

Under light illumination, the generated electrons-holes pairs are directly separated by the internal electrical fields which yield a photocurrent density j_{ph} . Two types of electrical fields are produced; one at the depletion region of the MIS contact and the other field is located at the contact depletion region of semiconductor 1 and semiconductor 2.

Figure 2 shows the band diagram of $SnO_2/SiO_2/GaInP/GaAs$ solar cell under illumination and at equilibrium. The insulating layer inserted between the metal and the semiconductor leads to the decrease of the thermoelectronic current as a result of the higher Schottky barrier. Concerning the $Ga_{1-x}In_xP / GaAs$ interface, we have noticed that the two semiconductors have different conduction band energies and valence band energies.

The electric potential difference V of the illuminated solar device is the sum of two components: V_i , generated at the insulating layer and V_s , produced at the depletion region of the semiconductor. The difference of potential is then $V=V_s+V_i$. The voltage V_i heightens the barrier between SnO_2 and $GaInP$ which will make difficult for electrons to pass through by thermal effect $B^*=B_n+V_i$. A higher barrier means that tunnel effect is the common mechanism for electron to get through the insulating layer. The current density in the $SnO_2/SiO_2/GaInP$ structure is: $J=J_{TH}-J_{TE}$. Thermoelectronic current density is given by:

$$j_{TE} = j_s \left(e^{\frac{eV}{kT}} - 1 \right) \quad (2)$$

and the saturation current :

$$j_s = A_e^* T^2 e^{-\left(\frac{eB_n^*}{kT}\right)} e^{-(\delta \times \sqrt{\chi_e})} \quad (3)$$

where ,

δ : thickness of insulating layer

χ_e : electron in affinity.

$$B_n = YB_0 + (1 - Y)(E_{g-st} - \Phi_0) \quad (4)$$

Φ_0 :Level measured from the peak of the valence band to the highest occupied interface level. In general, this energy is equal to $(E_g/3)$ [13].

E_{g-st} : strain gap [14]

International Journal of Advanced Research in Electrical, Electronics and Instrumentation Engineering

(An ISO 3297: 2007 Certified Organization)

Vol. 3, Issue 1, January 2014

Y: denotes the influence of the interface states on the Schottky barrier.

B_0 : Schottky barrier.

Minority carrier diffusion current is given by:

$$j_{dif} = j_0 \left(e^{\frac{qV_{bi}}{KT}} - 1 \right) \quad (5)$$

The diffusion voltage in the first loading area V_{bi} is given by $=B_0 - V_n$

where V_n represents the voltage difference between conduction band and Fermi level.

The current resulting from the passage of holes generated in the semiconductor and moving through the insulating layer to the metal by tunnel effect is given by the equation below:

$$j_{TH} = j_{ph} - j_0 \left[e^{\frac{q\Delta}{KT}} e^{\frac{qV_s}{KT}} - 1 \right] \quad (6)$$

$$\Delta = E_{g-st} - B_n^* - E_{fh} \quad (7)$$

$$V_s = \gamma V - \left(\frac{\gamma\delta}{\epsilon_i} \right) \sqrt{2qN_d\epsilon_s} (\sqrt{V_{bi}} - \sqrt{(V_{bi} - V_s)}) \quad (8)$$

ϵ_i : Insulating layer dielectric constant.

D_s : Interface state density

q : Electron charge.

N_d : Bulkdonordensity.

ϵ_s : Dielectricconstant of the semiconductor.

$$E_{fh} = \frac{KT}{q} \ln \frac{A_{TH}^* T^2 \exp\left[-\left(\chi_h^{1/2} \cdot \delta\right) + j_0 \exp\left[\frac{q}{KT}(E_{g-st} - B_n + V_s)\right]}{j_{ph} + j_0 + A_{TH}^* T^2 \exp\left[-\frac{q}{KT}(E_{g-st} - B_n - V_i) + \chi_h^{1/2} \cdot \delta\right]} \quad (9)$$

A_{TH}^* : Holes Richardson constant ($32A/cm^2K^2$)

χ_h : GaInP semiconductor holes affinity.

D_p : Holes diffusion constant.

L_p : Holes diffusion length.

V_{bi} : Diffusion volt agein w_l

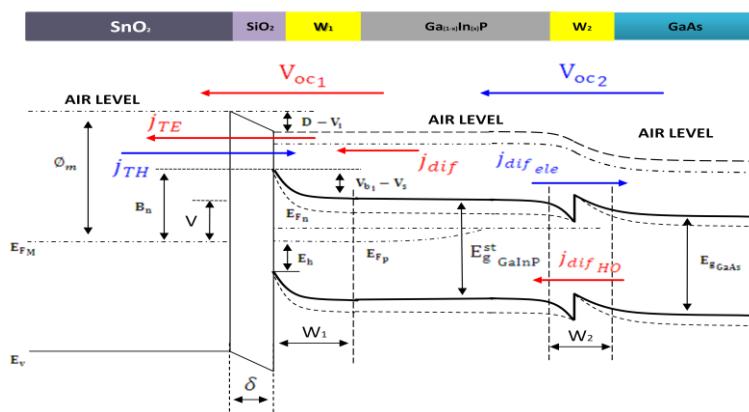


Fig. 2 Band diagram of the solar cell $SnO_2/SiO_2/GaInP/GaAs$ under illumination



International Journal of Advanced Research in Electrical, Electronics and Instrumentation Engineering

(An ISO 3297: 2007 Certified Organization)

Vol. 3, Issue 1, January 2014

IV. ELECTRICAL CHARACTERISTICS OF THE SnO₂/SiO₂/GaInP/GaAs SOLAR CELL

In the electrical characterization of solar cells, we have to extract Current-Voltage J(V), curves under illumination condition and calculate the maximum power delivered by the device and its light conversion efficiency. The current density of the structure is given by the equation:

$$j = j_{ph} - j_0 \left[e^{\left(\frac{q\Delta}{KT}\right)} e^{\left(\frac{qV_s}{KT}\right)} - 1 \right] - j_s \left[e^{\frac{eV}{KT}} - 1 \right] \quad (10)$$

The short-circuit current (j_{sc}) of the solar cell is expressed:

$$j_{sc} = j_{ph} - j_s \left[e^{\left(\frac{q\alpha\Delta}{KT}\right)} - 1 \right] - j_0 \left[e^{\frac{q(\Delta+\alpha\Delta)}{KT}} - 1 \right] \quad (11)$$

α : absorption coefficient of the semiconductor.

Open-circuit voltage V_{oc} of the solar cell is the sum of two voltages : $V_{oc} = V_{oc1} + V_{oc2}$.

V_{oc1} of SnO₂/SiO₂/GaInP structure is given by:

$$V_{oc1} = \frac{KT}{q} \ln \frac{j_{ph} + j_0 + j_s}{j_0 \exp [q(\Delta + \alpha\Delta)/KT] + j_s \exp (q\alpha\Delta /KT)} \quad (12)$$

V_{oc2} of the Ga_(1-x)In_xP/GaAs heterojunction structure is given by:

$$V_{oc2} = \frac{E_{g-st}}{q} - \frac{KT}{q} \ln \left(\frac{j_0}{j_{cc}} \right) \quad (13)$$

The photocurrent density crossing the MIS device is expressed by the equation below [15]:

$$j_{ph} = q \int_{\lambda_1}^{\lambda_2} F(\lambda) QE(\lambda) d\lambda \quad (14)$$

$F(\lambda)$: is the solar spectrum AMG1.5, λ_1 and λ_2 are wavelengths limits of absorbed solar spectrum. Taking into account the multiple reflections of light in the front and rear surfaces of the solar cell, optical electron-hole pair's generation rate is expressed in the following:

$$QE(\lambda) = [1 - R(\lambda)] \times e^{\{-\sum_{i=1}^2 \alpha_i z_i\}} \times [1 - e^{(-\alpha_{GaAs} L_{GaAs} - hc_{GaInP} \alpha_{GaInP})}] \quad (15)$$

Where $R(\lambda)$ is the surface spectrum reflectivity, the first exponential factor results from the attenuation of light in the precedent layers of the cell, α_i and z_i are respectively the absorption coefficient and the width of the precedent layers. It is noted that in our case, the upper layers are SnO₂ and SiO₂ which possess an absorption coefficient ($\alpha_i = 0$), α_{GaAs} and L_{GaAs} are the absorption coefficient and the width of the bulk material GaAs, α_{GaInP} and hc_{GaInP} are respectively the absorption coefficient and the width of the top lattice layer.

V. RESULTS AND DISCUSSION

Figure 3 shows the variation of the band energy gap vs Indium content. We have noticed that the gap decreases with increasing indium concentration whereas the strain (ϵ) decreases. For In concentration $x=0.48$ (lattice matching), the gap equals 1.73eV but for $x > 0.48$ the uniaxial compression gap is less than à 1.73eV with the strain $\epsilon > 0$. In the opposite, for $x < 0.48$, extensive strain is superior to 1.73 eV with $\epsilon < 0$. An example given is for $x=0.90$, the strain is $\epsilon = 2.98\%$ with the strain gap being $E_{gh-st} = 1.46eV$. We have maximum structure absorption in the case of a compressive strain as found elsewhere [16].

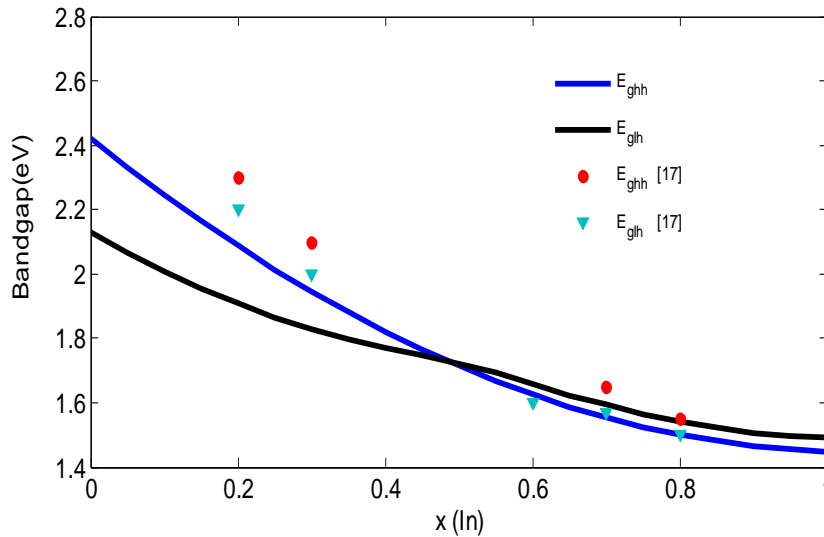


Fig.3 Bandgap variation as a function of the composition of indium

Figure 4 shows the variation the absorption with incident light energy $h\nu$. The absorption increases with higher Indium content. In the case we have a compressive constraint; the absorption is more significant than the case of a lattice match in gand extensive strain. For example, if $\epsilon=3.3\%$ the maximum absorption is $\alpha_{\max}=2.35 \cdot 10^5 \text{ cm}^{-1}$ but diminishes to $\alpha_{\max}=7.76 \cdot 10^4 \text{ cm}^{-1}$ for $\epsilon=-2.53\%$. That is a lattice matching-related increase of $\Delta\alpha_{\max}=1.44 \cdot 10^5 \text{ cm}^{-1}$.

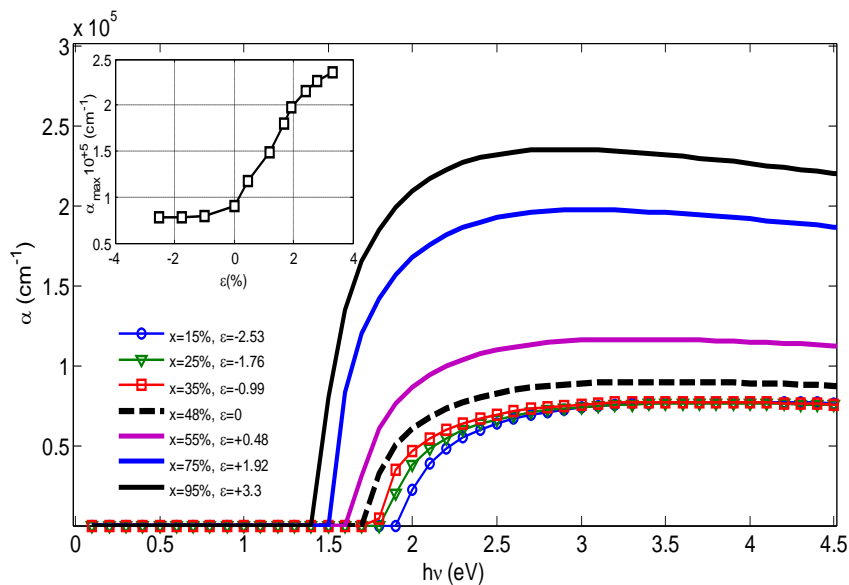


Fig 4 Absorption variation of GaInP structure as a function of the incident energy for different indium concentrations

In figure 5, we show the J(V) characteristics for different In concentration. For higher In concentrations, we notice that current density (J_{cc}) decreases while the open circuit voltage (V_{oc}) increase. The opposite happens in an extensive strain case ($\epsilon < 0$), J_{cc} is at a maximum and V_{oc} is minimal. The opposite effect is obtained for a compressive strain ($\epsilon > 0$) and where we can see that he fill factor (FF) increases.

International Journal of Advanced Research in Electrical, Electronics and Instrumentation Engineering

(An ISO 3297: 2007 Certified Organization)

Vol. 3, Issue 1, January 2014

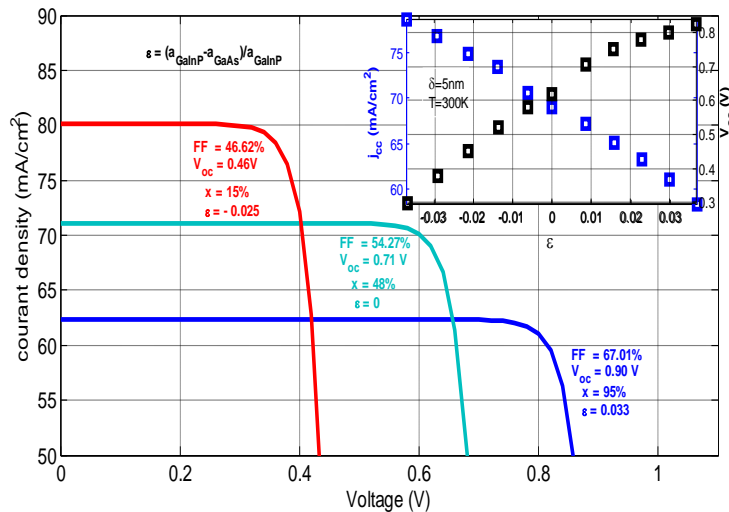


Fig. 5 J(V) characteristic for various indium concentrations, voltage variation (V_{oc}) and the current density (J_{cc}) as a function of strain (ϵ)

Figure 6 shows the variation of the structure power with the voltage. The maximum power delivered by the solar cell augments with higher compressive strain and lowers with an extensive one. For example, in the case of lattice matching ($\epsilon=0$), the maximal power amounts to 42.8mW but if we increase the strain to 3.3% the power reaches 48.83 mW that is an increase of $\Delta P_{max}=6.03mW$.

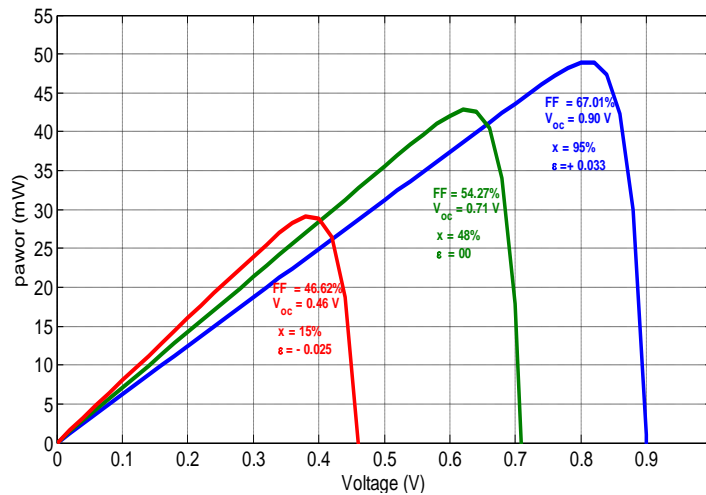


Fig.6 P(V) characteristic for various indium concentrations

Figure 7 depicts the efficiency (η) evolution of the GaInP/GaAs structure vs the strain ϵ . It is clearly seen that η increases when the strain increases. The solar cell efficiency is maximum when $\epsilon>0$ and is higher for thicker SiO_2 insulating layers. For a deformation of 3.3% and a thickness of $\delta= 50\text{\AA}$ we will have an efficiency of 26.8%. For example, if we consider a GaInP/GaAs structure with a 50\AA thick insulating layer and a deformation $\epsilon=1.21\%$, having an efficiency $\eta=23.17\%$, raising the deformation to $\epsilon=2.98\%$ will raise η to 26.6% the is a relative amelioration of $\Delta\eta= 3.43\%$. If we keep the deformation constant at $\epsilon=1.21\%$ and let the SiO_2 insulating layer thickness vary between 10 and 50\AA , the efficiency get boosted by $\Delta\eta=6.97\%$.

International Journal of Advanced Research in Electrical, Electronics and Instrumentation Engineering

(An ISO 3297: 2007 Certified Organization)

Vol. 3, Issue 1, January 2014

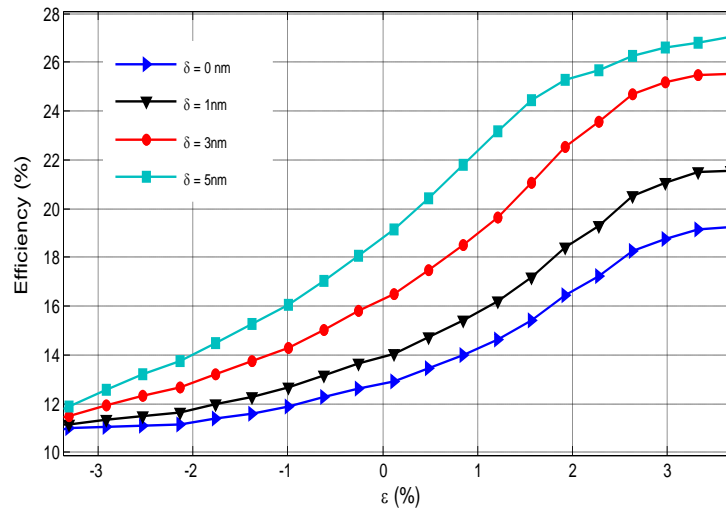


Fig.7 Efficiency variation as a function of the strain ϵ for different thicknesses of the insulating layer SiO_2

Figure 8 represents the variation of the quantum efficiency (EQE) vs wavelength where we can see that EQE of the GaInP structure reaches 92%. The width of the absorption becomes larger when the strain varies. For an extensive strain of $\epsilon = -0.025$, we notice that the absorption width varies between 310 to 520nm. In a lattice matched case, the width is larger and varies between 310 to 710nm. In the opposite situation, where we have a compressive strain ($\epsilon = +0.033$), the absorption width varies from 310 to 860nm. Our structure demonstrates the ability to turn more light into current and obtain higher efficiency by modifying the strain value and SiO_2 insulating layer thickness.

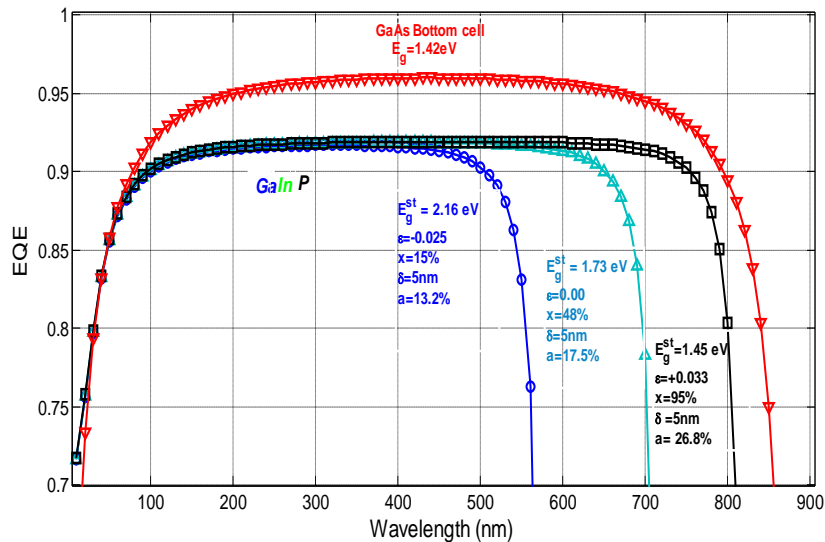


Fig. 8 Variation of the quantum efficiency as a function of wavelength for different indium concentrations

VI. CONCLUSION

In our study, it has been shown the influence of the $\text{Ga}_{1-x}\text{In}_x\text{P}/\text{GaAs}$ structure strain and SiO_2 insulating layer thickness (δ) on the solar cell light conversion efficiency. We have demonstrated that the compressive strain influences considerably and enhances the absorption, quantum efficiency and the efficiency. We noticed that a thicker SiO_2 insulating layer ameliorates the efficiency (η). Our findings show that for a compressive strain of 3.3% and SiO_2 thickness $\delta = 5\text{nm}$, the efficiency is $\sim 27\%$ whereas EQE reaches 92% in the spectral range 310-860nm. These results



International Journal of Advanced Research in Electrical, Electronics and Instrumentation Engineering

(An ISO 3297: 2007 Certified Organization)

Vol. 3, Issue 1, January 2014

show the effects of insulating layer thickness and strain parameters and their role in optimizing multi-junction and quantum multiwell structures.

REFERENCES

- [1] S. W. Zeng, B. P. Zhang, J. WSun, J. F. Cai, C. Chen and J. Z. Yu, "Substantial photo-response of InGaN p-i-n homojunction solar cells", *Semicond. Sci. Technol.* 24, 055009-4, 2009.
- [2] X. Chen, K. D. Matthews, D. Hao, W. J. Schaff, L. F. Eastman, "Growth, fabrication, and characterization of InGaN solar cells", *physica status solidi*, Volume 205, Issue 5, pp.1103–1105, 2008.
- [3] J. Wu, W. Walukiewicz, K. M. Yu, J. W. Ager III, E. E. Haller, H. Lu, W. J. Schaff, "Small bandgap bowing in $\text{In}_{1-x}\text{Ga}_x\text{N}$ alloys", *Appl. Phys.Lett.*80, pp. 4741–4743, 2002.
- [4] J. Wu, W. Walukiewicz, K. M. Yu, W. Shan, J. W.Ager III, E. E. Haller, H. Lu,W. J. Schaff, W. K. Metzger, S. Kurtz, "Superiorradiation resistance of $\text{In}_{1-x}\text{Ga}_x\text{N}$ alloys: Full-solar spectrum photovoltaic material system", *J.Appl. Phys.*94, pp. 6477–6482, 2003.
- [5] R. W. Hoffman JR., N.S. Fatemi, M.A. Stan, P. Jenkins, V.G. Weizer, D.A. Scheiman and D.J. Brinker, "High efficient InGaAs-on-GaAs devices for monolithic multi-junction solar cell applications," in *Proc. 2nd WCPEC*, Vienna, Austria, pp. 3604–3608, 1998.
- [6] T. Uchida, H. Kurakake, H. Soda, and S. Yamazaki, "A 1.3 μm strained quantum well laser on a graded InGaAs buffer with a GaAs substrate," *J. Electron. Mater.*, vol. 12 .581, 1996.
- [7] F. Dimroth, U. Schubert, and A. W. Bett, "25.5% Efficient $\text{Ga}_{0.35}\text{In}_{0.65}\text{P}/\text{Ga}_{0.83}\text{In}_{0.17}\text{P}$ Tandem Solar Cells Grown on GaAs Substrates", *IEEE Electron Device Letters*, vol. 21, n°. 5, pp. 209 – 211, 2000.
- [8] T. Takamoto, T. Agui, E. Ikeda, H. Kurita, "High efficiency InGaP=In0:01Ga0:99As tandem solar cells lattice matched to Ge substrates, *Sol. Energy Mater. Sol. Cells* 66, 511,2001.
- [9] N. J. Ekins-Daukes, D. B. Bushnell, J. P. Connolly, K. W. J. Barnham, M. Mazzer, J.S. Roberts, G. Hill, R. Airey, "Strain-balanced quantum well solar cells", *Physica E* 14, pp. 132–135, 2002.
- [10] F. Thieblemont, "Recherche sur les Cellules Photovoltaïques Métal/Isolant Organique/Semi-Conducteur", *Ambassade de France en Israel Service de Coopération & d'Action Culturelle*, pp. 2-13, 2008.
- [11] C.F. Hector Cotal, "III–V Multijunction Solar Cells for Concentrating Photovoltaics". *Energy & Environmental Science* , pp. 174–192, 2008.
- [12] G. Ghione, "Semiconductor Devices for High-Speed Optoelectronics", *Politecnico Ditorino,Italy,Cambridge University Press*, 2009.
- [13] R. Z. Gueddim, "Optimisation d'un Tandem Mécanique de Cellules Solaires($\text{AlGaAs}/\text{GaAs}$) / ($\text{SnO}_2/\text{SiO}_2/\text{Si}$)", *RevEnerg*, pp. 87-93, 2002.
- [14] A. Aissat, S. Nacer, M. Bensebti, J.P. Vilcot, "Investigation on the emission wavelength of GaInNAs/GaAs strained compressive quantum wells on GaAs substrates", *Microelectronics Journal* 39 pp. 63–66, 2008.
- [15] C. N. Liulei, "Temperature Dependent Spectral Response Characteristic of III-VCompound Tandem Cell", *Chinese Science Bulletin*, pp. 353-357, 2009.
- [16] M. A. Steiner,L. Bhusal, J. F. Geisz, A. G. Norman, M. J. Romero, W. J. Olavarria, Y. Zhang, and A. Mascarenhas, "CuPt ordering in high bandgap Ga_{1-x}P alloys on relaxed GaAsP step grades", *Journal of Applied Physics* 106, 063525-5, 2009.